Large magnetic entropy change and magnetoresistance in a $Ni_{41}Co_9Mn_{40}Sn_{10}$ magnetic shape memory alloy

L. Huang[1,2], D. Y. Cong[1,a)], L. Ma[3], Z. H. Nie[2], M. G. Wang[4], Z. L. Wang[2], H. L. Suo[3], Y. Ren[5], and Y. D. Wang[1,b)]

[1] *State Key Laboratory for Advanced Metals and Materials, University of Science and Technology Beijing, No. 30 Xueyuan Rd, Haidian District, Beijing 100083, People's Republic of China*

[2] *School of Materials Science and Engineering, Beijing Institute of Technology, Beijing 100081, People's Republic of China*

[3] *College of Materials Science and Engineering, Beijing University of Technology, Beijing 100124, People's Republic of China*

[4] *College of Sciences, Northeastern University, Shenyang 110819, People's Republic of China*

[5] *X-ray Science Division, Argonne National Laboratory, Argonne, IL 60439, USA*

[a)]Email: dycong@ustb.edu.cn

[b)]Email: ydwang@ustb.edu.cn

Abstract

We report the simultaneously obtained large magnetoresitance and large magnetic entropy change in a $Ni_{41}Co_9Mn_{40}Sn_{10}$ magnetic shape memory alloy. A large magnetoresitance of 53.8% (under 5T) and a large magnetic entropy change of 31.9 J/(kg K) (under 5T) were achieved. Both of these values are among the highest values reported so far in Ni-Mn-Sn-based Heusler alloys. The large magnetic entropy change, closely related to the structural entropy change, is attributed to the large unit cell volume change across martensitic transformation as revealed by our in-situ high-energy X-ray diffraction experiment. Furthermore, this $Ni_{41}Co_9Mn_{40}Sn_{10}$ alloy exhibits good mechanical properties. The combination of large magnetoresitance, large magnetic entropy change, and good mechanical properties, as well as low cost and non-toxicity, makes this alloy a promising candidate for multifunctional applications.

Keywords: Magnetocaloric effect; Magnetoresistance; Magnetic shape memory alloy

I. INTRODUCTION

In the last decade, NiMn-based Ni–(Co)–Mn–X (X = In, Sn, Sb) Heusler alloys have gained much attention due to their multifunctionalities, such as magnetic shape memory effect,[1,2] magnetocaloric effect,[3,4] magnetoresistance,[5,6], magnetothermal conductivity[7] and elastocaloric effect.[8] Such properties originate from the first order magnetostructural transformation from high-temperature austenite phase to low-temperature martensite phase. It is believed that these above mentioned multifunctional properties can lead to potential applications in novel actuators, high-efficiency sensors and environment-friendly magnetic refrigerators.

During martensitic transformation the ferromagnetic austenite transforms into weak magnetic martensite, and thus a large magnetization difference (ΔM) can be obtained. Applying a magnetic field at a temperature close to the reverse transformation temperature could induce the transformation from weak magnetic martensite to ferromagnetic austenite and therefore the magnetocaloric effect could be observed. According to the Clausius-Clapeyron relation,[1] a large ΔM is beneficial to the achievement of large magnetic entropy change. In Co-doped Ni–Mn–X (X = In, Sn and Sb) alloys where large magnetic entropy change is usually obtained, the large ΔM is attributed to the Co substitution for Ni turning the magnetic moments of Mn atoms into a ferromagnetic ordering instead of antiferromagnetic one.[9] Since the electrical resistivity of austenite and martensite is significantly different, during magnetic-field-induced transformation the electrical resistivity changes, leading to the large magnetoresistance. The large electrical resistivity difference ($\Delta\rho$) is related with the variation of the density of the electronic state in the vicinity of the Fermi surface during phase transition.[9, 10]

For potential applications of Ni–(Co)–Mn–X (X = In, Sn, Sb) as multifunctional alloys, it is strongly desirable to simultaneously obtain large magnetocaloric effect and large magnetoresistance in a single alloy. However, in most studies only one remarkable property, either large magnetocaloric effect or large magnetoresistance, could be achieved in a certain alloy.[3,5] Reports on both large magnetocaloric effect and large magnetoresistance are very scarce. On the other hand, in addition to good

functional properties, the machinability of the alloys should be taken into account for practical applications.[11] However, little and scattered information concerning the mechanical properties[12] of the Ni–(Co)–Mn–X (X = In, Sn, Sb) multifunctional alloys could be found in the literature.

In this work, we report both large magnetic entropy change, 31.9 J/(kg K) under 5T, and large magnetoresistance, 53.8% under 5T, in a $Ni_{41}Co_9Mn_{40}Sn_{10}$ Heusler alloy. Each of these values is among the highest values reported in literature in which, however, only one of these two exceptional properties was obtained. Moreover, good mechanical properties are achieved in the studied alloy. The origin of the large magnetic entropy change is interpreted in terms of unit cell volume change across martensitic transformation.

II. EXPERIMENTAL

The polycrystalline ingot with composition of $Ni_{41}Co_9Mn_{40}Sn_{10}$ (at.%) was prepared by repeated melting in an arc furnace under argon atmosphere. Subsequently it was sealed in an evacuated quartz tube and annealed at 1223 K for 9 h followed by water quenching to ensure homogeneity. The phase transformation temperatures were measured by differential scanning calorimetry (DSC) in the temperature range of 223-473 K with cooling and heating rates of 10 K/min; the martensitic and austenitic transformation start and finish temperatures, M_s, M_f, A_s and A_f, are determined to be 353 K, 334 K, 354 K, and 371 K, respectively. The entropy change (ΔS) across the transformation is determined from the DSC data to be 32.1 J/(kg K). Magnetic measurements and electrical resistivity measurements were performed in a physical property measurement system (PPMS, Quantum Design) with a magnetic field up to 14 T. Temperature-dependent in-situ synchrotron high-energy X-ray diffraction (HEXRD) experiments were carried out at the 11-ID-C beamline at the Advanced Photon Source, Argonne National Laboratory, USA. A monochromatic X-ray beam with a wavelength of 0.10804 Å was used. The diffraction Debye rings were collected by a two-dimensional (2D) image plate detector. Conventional transmission electron microscopy (TEM) experiment was performed to study the crystal structure of

martensite at room temperature. Thin foil samples for TEM observation were first mechanically ground to ~80 μm in thickness, followed by dimpling and ion-milling at 5 kV. Compressive test of a specimen of Φ3×6 mm^3 was conducted using a mechanical testing machine (Instron 5966) at room temperature.

III. RESULTS AND DISCUSSION

Fig.1 shows the temperature dependence of magnetization [$M(T)$ curve] measured under 0.0T and 4T for the $Ni_{41}Co_9Mn_{40}Sn_{10}$ alloy. From the $M(T)$ curve under 0.01 T, M_s, M_f, A_s and A_f, are determined to be 351 K, 339 K, 357 K, and 368 K, respectively, which is consistent with the DSC results. As seen from Fig. 1 and taking into account the characteristics of the isothermal magnetization curves [$M(H)$ curves] at different temperatures (see Fig. 3(a)), the high-temperature austenite shows ferromagnetic feature while the low-temperature martensite is in a weak magnetic state. Consequently, there is a large magnetization difference ($\Delta M \approx 90$ emu/g) between the two phases across martensitic transformation. Under the high magnetic field of 4 T, all of the characteristic transformation temperatures are shifted to lower temperatures. The A_s temperature is decreased by 11 K, with the rate of $\Delta A_s/\mu_0\Delta H \approx 2.75$ K/T. According to the Clausius-Clapeyron relation,[1] $\Delta T/\mu_0\Delta H \approx (\Delta M/\Delta S)$, where ΔT is the decrease of transformation temperature induced by the magnetic field change ΔH. With the ΔM and ΔS (as determined from DSC measurement) values mentioned above, $\Delta M/\Delta S$ (and hence $\Delta T/\mu_0\Delta H$) is calculated to be ~2.80 K/T, which is in good agreement with the experimental $\Delta A_s/\mu_0\Delta H$ value (~2.75 K/T).

To evaluate the magnetoresistance of the alloy, the temperature dependence of the electrical resistivity was measured under 0T and 5T during heating, as shown in the inset of Fig. 2. The magnetoresistance, MR, is calculated as $(\rho(H)-\rho(0))/\rho(0)$, where $\rho(H)$ is the resistivity under magnetic field and $\rho(0)$ is the resistivity at zero magnetic field.[13,14] The temperature dependence of MR under 5 T is plotted in Fig. 2. It can be seen that the negative peak value of MR is about 53.8% at 355 K under 5T, which is significantly larger than that of other Ni-(Co)-Mn-Sn materials under the same

field,[15-17] and it is comparable to that of the giant magnetoresistance materials such as $Ni_{50}Mn_{34}In_{16}$ (*MR*=64%, 5T)[5] and $Ni_{41}Co_9Mn_{39}Sb_{11}$ (*MR*=60%, 5T).[18] The large *MR* value for the presently studied $Ni_{41}Co_9Mn_{40}Sn_{10}$ alloy stems from the tremendous difference between austenite and martensite in resistivity and the great sensitivity of transformation temperatures to magnetic field (almost complete magnetic-field-induced transformation from martensite to austenite occurs at 355 K under 5 T).

In order to assess the magnetocaloric effect, the *M*(*H)* curves at different temperatures close to austenitic transformation temperatures were measured, which are shown in Fig. 3(a). Before each measurement, the sample was first cooled to 250 K (< M_f) to ensure the same initial state of a fully transformed martensite and then heated to the measurement temperature. This is to avoid the effect of possible residual field-induced austenite owing to the incomplete transformation from austenite to martensite during decreasing magnetic field in the previous measurement which could lead to an artificial magnetic entropy change value.[19-21] The curves were recorded during both increasing and decreasing magnetic fields, but for clarity only those recorded during increasing fields are shown in Fig. 3a. The magnetic entropy change ΔS_m was calculated using the Maxwell relation from the *M*(*H)* curves,[3]

$$\Delta S_m = S_m(T,H) - S_m(T,0) = \int_0^{\mu_0 H} \frac{\partial M}{\partial T} d(\mu_0 H). \quad (1)$$

The temperature dependence of the calculated ΔS_m at different magnetic fields is demonstrated in Fig. 3(b). It can be seen that the maximum value of ΔS_m under 5 T is ~31.9 J/(kg K), which is obtained around 358 K. It should be pointed out that at temperatures around 358 K, applying a magnetic field of 5T is sufficient to induce the complete transformation from martensite to austenite, as confirmed by the *M*(*H)* curves shown in Fig. 3(a). In this case, the maximum achievable ΔS_m should be close to the entropy change determined from the DSC measurement. Indeed, a good agreement between these two values (~31.9 and 32.1 J/(kg K)) is obtained. On the other hand, the ΔS_m values were also estimated with the Clausius-Clapeyron relation for first order phase transformation, $\Delta S_m \approx \Delta M(\mu_0 \Delta H/\Delta T)$ in which $\mu_0 \Delta H/\Delta T$ can

be obtained from the temperature dependence of the critical field for magnetic-field-induced transformation,[22] which can be determined from the *M*(*H)* curves in Fig. 3(a). The maximum value estimated with this relation is ~31.6 J/(kg K), which is consistent with the values calculated using the Maxwell relation and experimentally obtained from the DSC measurement. This confirms that our maximum ΔS_m value is reliable. The ΔS_m value of ~31.9 J/(kg K) (under 5 T) is among the largest values reported heretofore for Ni-Mn-Sn-based alloys. It should be noted that nearby or even higher ΔS_m values were also reported in literature.[12,23-26] However, in many of those studies[23,25,26] the *M*(*H)* curves were recorded during continuous heating which may lead to spurious spikes on the $\Delta S_m \sim T$ curve;[19,27,28] indeed, sharp peaks were present on the $\Delta S_m \sim T$ curve in some studies.[23,24] What is more, the ΔS_m values reported[12,23-26] were only obtained with the Maxwell equation and they were not compared with the results determined from DSC measurement or calculated from the Clausius-Clapeyron relation or from the temperature dependence of specific heat capacity under different magnetic fields. Therefore, the ΔS_m values reported therein may be questionable.

It is known that when magnetic-field-induced transformation is completely driven, the magnitude of the magnetic entropy change ΔS_m is closely related to that of the structural entropy change during phase transformation. The large ΔS_m obtained in our alloy is due to its large structural entropy change. To elucidate the origin of the large structural entropy change, in-situ HEXRD experiments were performed in the temperature range of 400-100 K which covers the martensitic transformation region. Fig.4 (a) and 4(b) show the HEXRD patterns collected at 400 K and 100 K, respectively. Careful analysis shows that at 400 K the sample is in the austenitic state and all the diffraction peaks can be well indexed according to the $L2_1$ cubic Heusler structure; at 100 K the sample shows a martensitic structure and the diffraction pattern can be well indexed according to the six-layered modulated (6M) monoclinic structure.[2] To confirm the crystal structure of martensite, TEM experiment was performed. Fig. 4(c) shows the selected area electron diffraction pattern (SAEDP) for martensite at room temperature, from which one can see that there are five extra

satellite spots (marked by the white arrows) between the main reflections, characteristic for the 6M martensitic structure.[29] This is consistent with the HEXRD result.

The temperature dependence of the lattice parameters and the unit cell volume of austenite and martensite are shown in Fig. 5(a) and 5(b). Considering the orientation relationship between austenite and martensite,[30] to examine the change of the lattice and unit cell volume during martensitic transformation the variation of $\sqrt{2}a_{\mathrm{M}}$, $\sqrt{2}c_{\mathrm{M}}/6$ and b_{M} (instead of a_{M}, c_{M} and b_{M}) [Fig. 5(a)] and the variation of $V_{\mathrm{M}}/3$ (instead of V_{M}) [Fig. 5(b)] are displayed in the figure for easy comparison with austenite. It can be seen that the lattice parameters of austenite (a_{A}) display a slight change with the variation of temperature. In contrast, the lattice parameters a_{M} and β angle [inset of Fig. 5(b)] of the 6M martensite increase obviously while b_{M} and c_{M} decrease with temperature decreasing in the range of 340-100 K. Strikingly, across martensitic transformation the lattice shrinks by 6.9% along the b_{M} axis and expands by 4.0% and 2.1% along a_{M} and c_{M}, respectively. Such lattice parameter changes lead to a significant unit cell volume contraction by 1.31% when austenite transforms to martensite. Recently, it was reported that for first order magnetostructural transformation the structural entropy change is proportional to the unit cell volume change across phase transformation;[31] the larger the unit cell volume change, the larger the structural entropy change. Therefore, the significant unit cell volume change (-1.31%) lies at the origin of the large structural entropy change and consequently large magnetic entropy change observed in the presently studied alloy. In fact, in the Fe-Rh,[32] Gd-Si-Ge[33] and La-Fe-Si[34] materials with large unit cell volume change (0.9%, 0.4%, 1.3%, respectively) during phase transformation, large magnetic entropy change was observed. Most remarkably, in the Mn-Co-Ge-B alloy with the large unit cell volume change of 4.0%,[31,35] giant magnetic entropy change of -47.3 J/kg K (under 5T) was recently discovered by Trung *et al*.[35] The correlation between the unit cell volume change and magnetic entropy change is instructive for predicting high-performance magnetocaloric materials from the crystallographic data.

It should be stressed that, for practical applications, the machinability of the multifunctional alloys is of equal importance to their functional properties.[11] Fig. 6 shows the compressive stress-strain curve of the studied $Ni_{41}Co_9Mn_{40}Sn_{10}$ alloy at room temperature. One can see that following the elastic deformation there is an obvious work hardening stage. The compressive strength is 845 MPa and the compressive strain reaches 4.5%. This compressive strain is significantly higher than that of other Ni-Mn-based Heusler alloys[12] with good functional properties. It should be noted that the high-performance Gd-Si-Ge and La-Fe-Si magnetocaloric materials are quite brittle,[11] even lack of any processing ability. The good mechanical properties of our alloy ensure good machinability so that it could be processed into the required shapes for potential applications.

IV. CONCLUSIONS

A large magnetic entropy change of 31.9 J/(kg K) under 5T and a large magnetoresitance of 53.8% under 5T were simultaneously obtained in a $Ni_{41}Co_9Mn_{40}Sn_{10}$ alloy. Each of these values is among the highest values reported to date for Ni-Mn-Sn-based alloys. The large magnetic entropy change is attributed to the large unit cell volume change across phase transformation as revealed by in-situ HEXRD experiments. Noteworthily, good mechanical properties were also achieved in this $Ni_{41}Co_9Mn_{40}Sn_{10}$ alloy. With no expensive or toxic elements, this alloy has low cost and it is environmentally friendly. All these merits make this alloy attractive for potential multifunctional applications.

ACKNOWLEDGMENTS

This work is supported by the National Basic Research Program of China (973 Program) under Contract No. 2012CB619405, the National Natural Science Foundation of China (Nos. 51471030 and 11305008), the National 863 Program of China (Grant No. 2015AA034101), the Fundamental Research Funds for the Central Universities (Nos. 06111023 and 06111020), the NPL, CAEP (Project No. 2013DB02), and the projects (Grant Nos. 2014Z-01 and 2014Z-02) from the State

Key Laboratory for Advanced Metals and Materials. Use of the Advanced Photon Source was supported by the U.S. Department of Energy, Office of Science, Office of Basic Energy Science, under Contract No. DE-AC02-06CH11357.

References

[1]R. Kainuma, Y. Imano, W. Ito, Y. Sutou, H. Morito, S. Okamoto, O. Kitakami, K. Oikawa, A. Fujita, T. Kanomata, and K. Ishida, Nature (London) **439**, 957 (2006).

[2]H. E. Karaca, I. Karaman, B. Basaran, Y. Ren, Y. I. Chumlyakov, and H. J. Maier, Adv. Funct. Mater. **19**, 983 (2009).

[3]T. Krenke, E. Duman, M. Acet, E. F. Wassermann, X. Moya, L. Mañosa, and A. Planes, Nat. Mater. **4**, 450 (2005).

[4]L. Huang, D. Y. Cong, H. L. Suo, and Y. D. Wang, Appl. Phys. Lett. **104**, 132407 (2014).

[5]V. K. Sharma, M. K. Chattopadhyay, K. H. B. Shaeb, A. Chouhan, and S. B. Roy, Appl. Phys. Lett. **89**, 222509 (2006).

[6]K. Koyama, H. Okada, K. Watanabe, T. Kanomata, R. Kainuma, K. Oikawa, W. Ito, and K. Ishida, Appl. Phys. Lett. **89**, 182510 (2006).

[7]B. Zhang, X. X. Zhang, S. Y. Yu, J. L. Chen, Z. X. Cao, and G. H. Wu, Appl. Phys. Lett. **91**, 012510 (2007).

[8]R. Millán-Solsona, E. Stern-Taulats, E. Vives, A. Planes, J. Sharma, A. Nayak, K. G. Suresh, and L. Mañosa, Appl. Phys. Lett. **105**, 241901(2014).

[9]S. Y. Yu, L. Ma, G. D. Liu, Z. H. Liu, J. L. Chen, Z. X. Cao, G. H. Wu, B. Zhang and X. X. Zhang, Appl. Phys. Lett. **90**, 242501 (2007).

[10]S. Y. Yu, Z. H. Liu, G. D. Liu, J. L. Chen, Z. X. Cao, G. H. Wu, B. Zhang and X. X. Zhang, Appl. Phys. Lett. **89**, 162503 (2006).

[11]J. Lyubina, R. Schäfer, N. Martin, L. Schultz, and O. Gutfleisch, Adv. Mater. **22**, 3735 (2010).

[12]Y. Zhang, J. Liu, Q. Zheng, J. Zhang, W. X. Xia, J. Du, and A. Yan. Scr. Mater. **75**, 26 (2014).

[13]H. C. Xuan, L. J. Shen, T. Tang, Q. Q. Cao, D. H. Wang, and Y. W. Du, Appl. Phys.

Lett. **100**, 172410 (2012).

[14]H. C. Xuan, Y. X. Zheng, S. C. Ma, Q. Q. Cao, D. H. Wang, and Y. W. Du, J. Appl. Phys. **108**,103920 (2010).

[15]S. Pramanick, S. Chatterjee, S. Giri, and S. Majumdar, Appl. Phys. Lett.**105**,112407 (2014).

[16]S. Singh and C. Biswas, Appl. Phys. Lett. **98**, 212101 (2011).

[17]J. Dubowik, K. Załeski, I. Goscianska, H. Głowinski,and A. Ehresmann, Appl. Phys. Lett. **100**, 162403 (2012).

[18]Z. D. Han, D. H. Wang, C. L. Zhang, H. C. Xuan, J. R. Zhang, B. X. Gu, and Y. W. Du, J. Appl. Phys. **104**, 053906 (2008).

[19]J. Liu, N. Scheerbaum, J. Lyubina, and O. Gutfleisch, Appl. Phys. Lett. **93**, 102512 (2008).

[20]D.Y. Cong, S. Roth, and L. Schultz, Acta Mater. **60**, 5335 (2012).

[21]E. K. Liu, W. H. Wang, F. Lin, W. Zhu, G. J. Li, J. L. Chen, H. W. Zhang, G. H. Wu, C. B. Jiang, H. B. Xu, and F. de Boer, Nat. Commun. **3**, 873 (2012).

[22]A. Giguère, M. Foldeaki, B. R. Gopal, R. Chahine, T. K. Bose, A. Frydman, and J. A. Barclay, Phys. Rev. Lett. **83**, 2262 (1999).

[23]S. E. Muthu, N. V. R. Rao, M. M. Raja, D. M. R. Kumar, D. M. Radheep and S. Arumugam, J. Phys. D: Appl. Phys. **43**, 425002 (2010).

[24]R. Das, S. Sarma, A. Perumal, and A. Srinivasan, J. Appl. Phys. **109**, 07A901 (2011).

[25]H. C. Xuan, K. X. Xie, D. H. Wang, Z. D. Han, C. L. Zhang, B. X. Gu, and Y. W. Du, Appl. Phys. Lett. **92**, 242506 (2008).

[26]L. H. Yang, H. Zhang, F. X. Hu, J. R. Sun, L. Q, Pan, and B. G. Shen, J. Alloys Compd. **588**, 46 (2014).

[27]M. Balli, D. Fruchart, D. Gignoux, and R. Zach, Appl. Phys. Lett. **95**, 072509 (2009).

[28]L. Chen, F. X. Hu, J. Wang, L. F. Bao, J. R. Sun, B. G. Shen, J. H. Yin, and L. Q. Pan, Appl. Phys. Lett. 101, 012401 (2012).

[29]H. F. Tian, J. B. Lu, L. Ma, H. L. Shi, H. X. Yang, G. H. Wu, and J. Q. Li, J. Appl.

Phys. **112**, 033904 (2012).

[30]P. J. Brown, J. Crangle, T. Kanomata, M. Matsumoto, K-U. Neumann, B. Ouladdiaf, and K. R. A. Ziebeck, J. Phys. Condens. Matter. **14,** 10159 (2002).

[31]K. A. Gschneidner, Jr. Y. Mudryka and V. K. Pecharsky, Scr. Mater. **67**, 572 (2012).

[32]P. A. Algarabel, M. R. Ibarra, C. Marquina, A. del Moral, J. Galibert, M. Iqbal, and S. Askenazy, Appl. Phys. Lett. **66**, 3061 (1995).

[33]L. Morellon, P. A. Algarabel, M. R. Ibarra, J. Blasco, B. Garcia-Landa, Z. Arnold, and F. Albertini, Phys. Rev. B **58**, R14721 (1998).

[34]F. Hu, B. Shen, J. Sun, G. Wang, and Z. Cheng, Appl. Phys. Lett. **50**, 826 (2002).

[35]N. T. Trung, L. Zhang, L. Car on, K. H. J. Buschow, and E. Brück, Appl. Phys. Lett. **96**, 172504 (2010).

Figure Captions

FIG. 1. M(T) curves measured under magnetic fields of 0.01 and 4T, respectively.

FIG. 2. Magnetoresistance as a function of temperature under 5 T. The inset shows the temperature dependence of resistivity during heating under magnetic fields of 0 and 5T, respectively.

FIG. 3. (a) M(H) curves measured at different temperatures close to the austenitic transformation temperatures. (b) The magnetic entropy change (ΔS_m) as a function of temperature at different magnetic fields.

FIG. 4. (a, b) High-energy X-ray diffraction patterns experimentally collected at 400 K (a) and 100K (b) corresponding to austenite (A) and martensite (M) phase, respectively. (c) Selected area electron diffraction pattern (SAEDP) for martensite at room temperature.

FIG. 5. Temperature dependence of the lattice parameters (a) and the unit cell volume (b) of austenite and martensite. The inset of (b) shows the β angle of the six-layered modulated monoclinic structure of martensite as a function of temperature.

FIG. 6. Compressive stress–strain curve measured at room temperature.

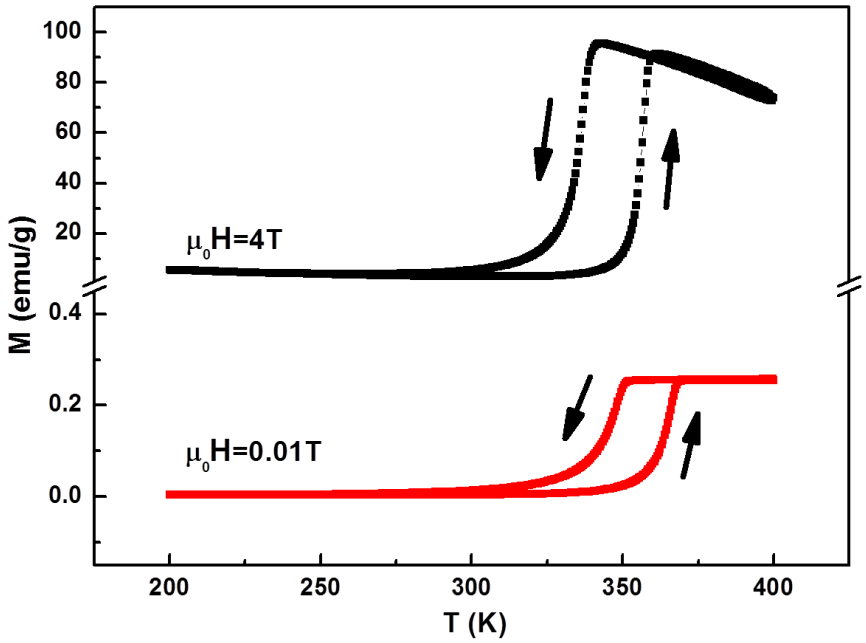

FIG. 1. M(T) curves measured under magnetic fields of 0.01 and 4T, respectively.

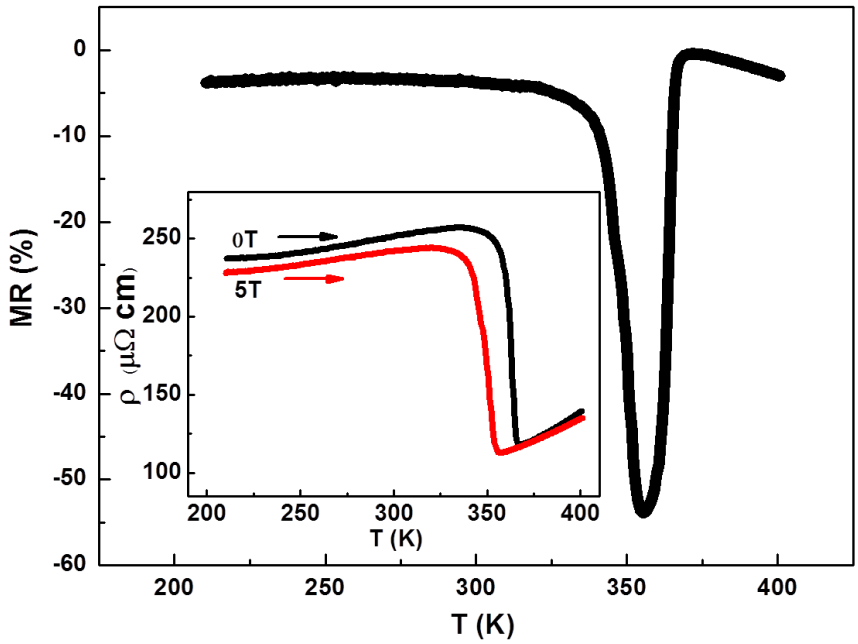

FIG. 2. Magnetoresistance as a function of temperature under 5 T. The inset shows the temperature dependence of resistivity during heating under magnetic fields of 0 and 5T, respectively.

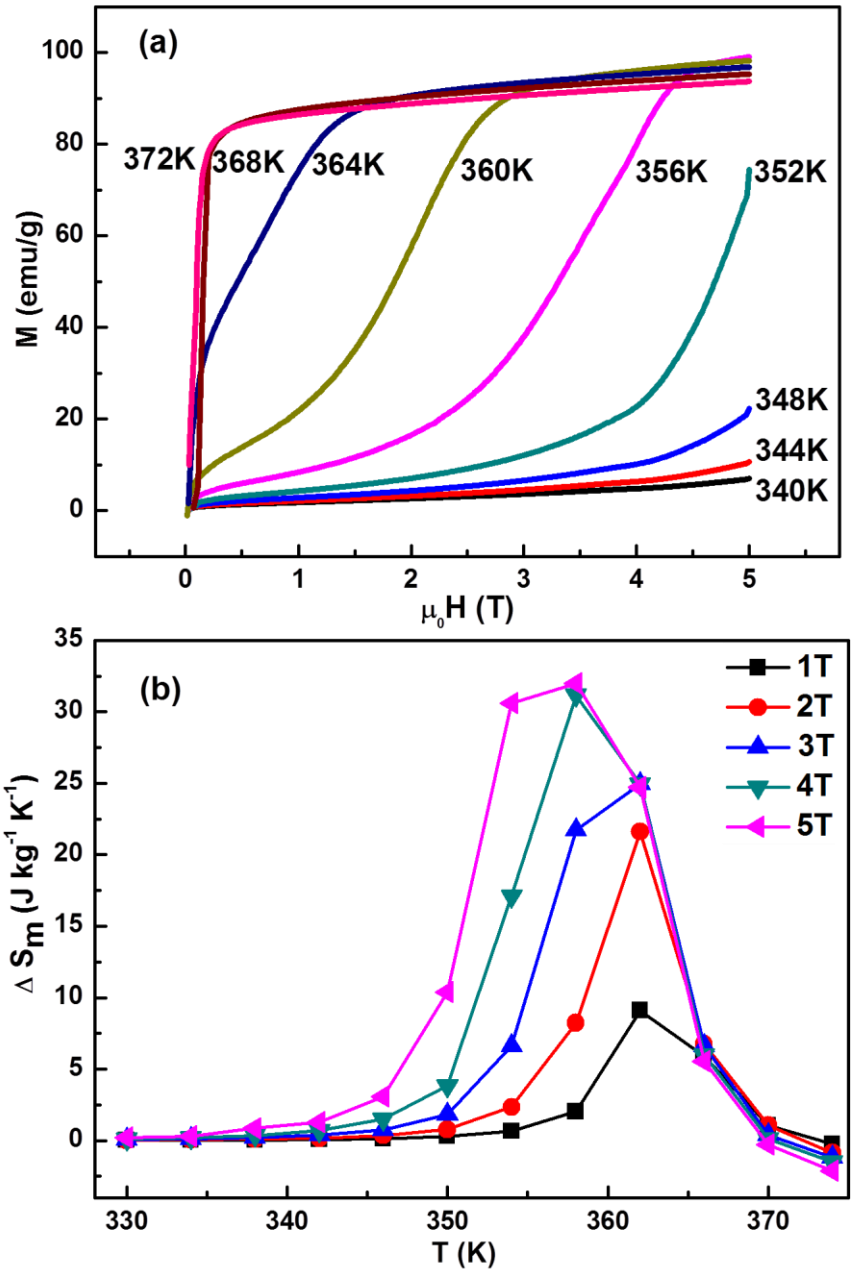

FIG. 3. (a) M(H) curves measured at different temperatures close to the austenitic transformation temperatures. (b) The magnetic entropy change (ΔS_m) as a function of temperature at different magnetic fields.

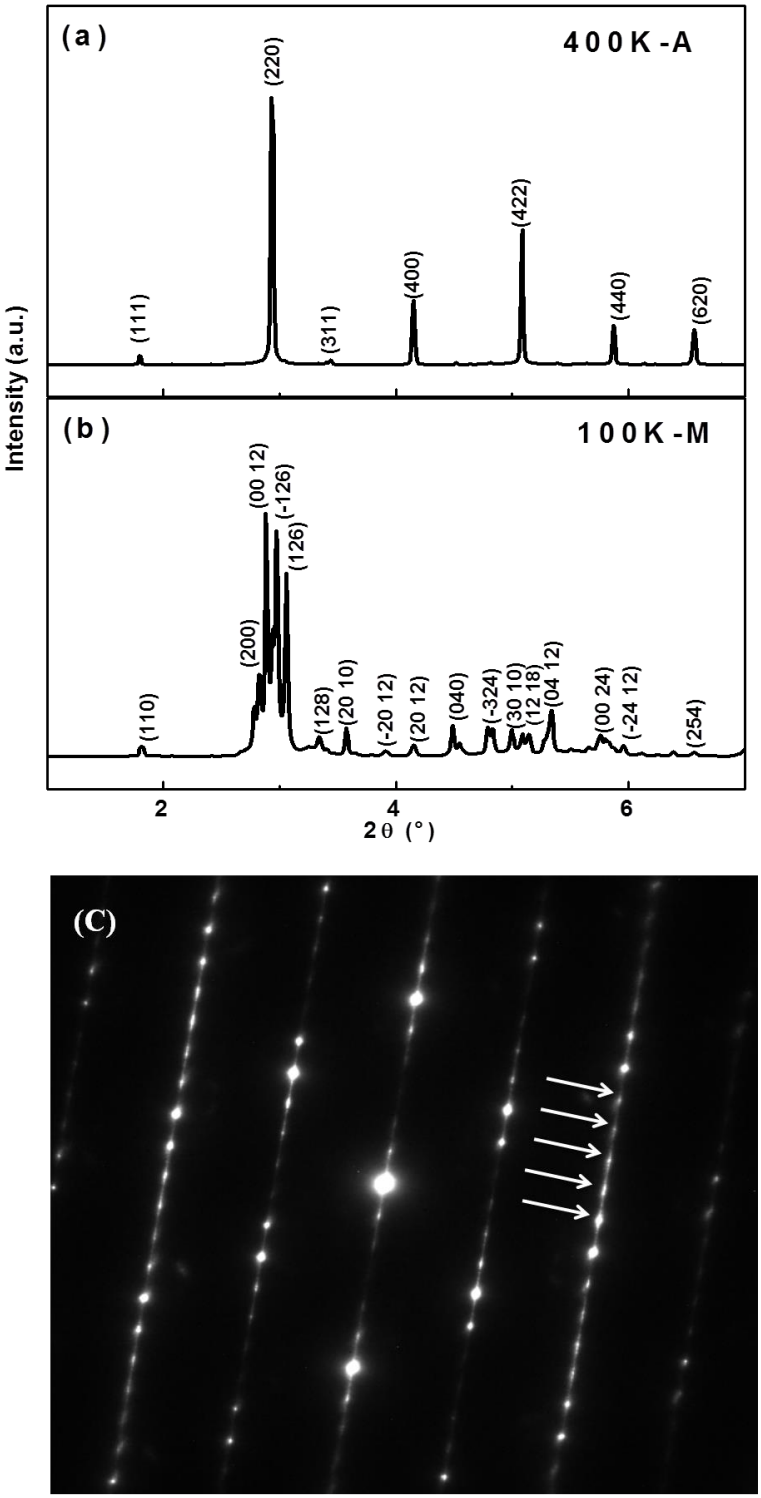

FIG. 4. (a, b) High-energy X-ray diffraction patterns experimentally collected at 400 K (a) and 100 K (b) corresponding to austenite (A) and martensite (M) phases, respectively. (c) Selected area electron diffraction pattern (SAEDP) for martensite at room temperature.

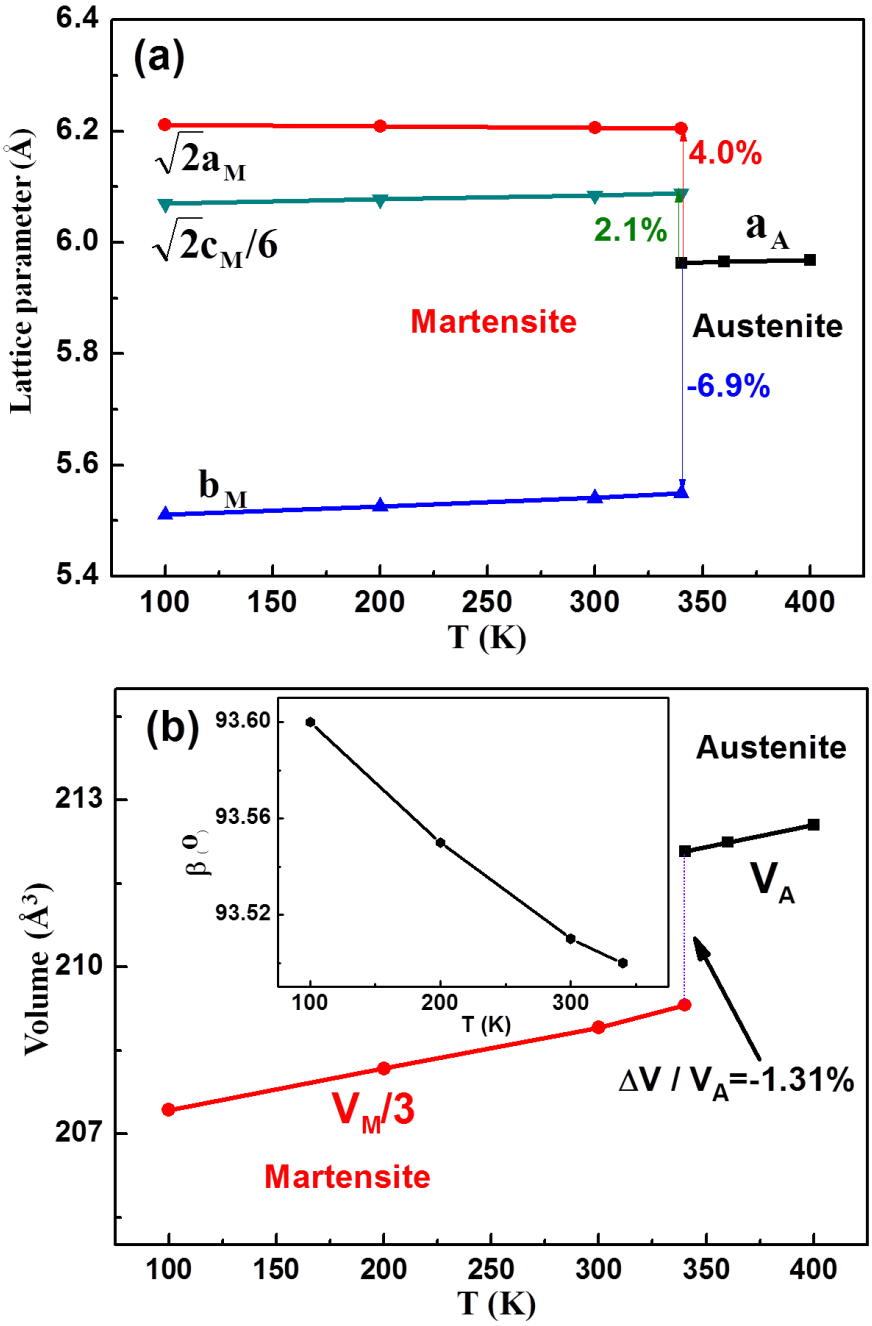

FIG. 5. Temperature dependence of the lattice parameters (a) and the unit cell volume (b) of austenite and martensite. The inset of (b) shows the β angle of the six-layered modulated monoclinic structure of martensite as a function of temperature.

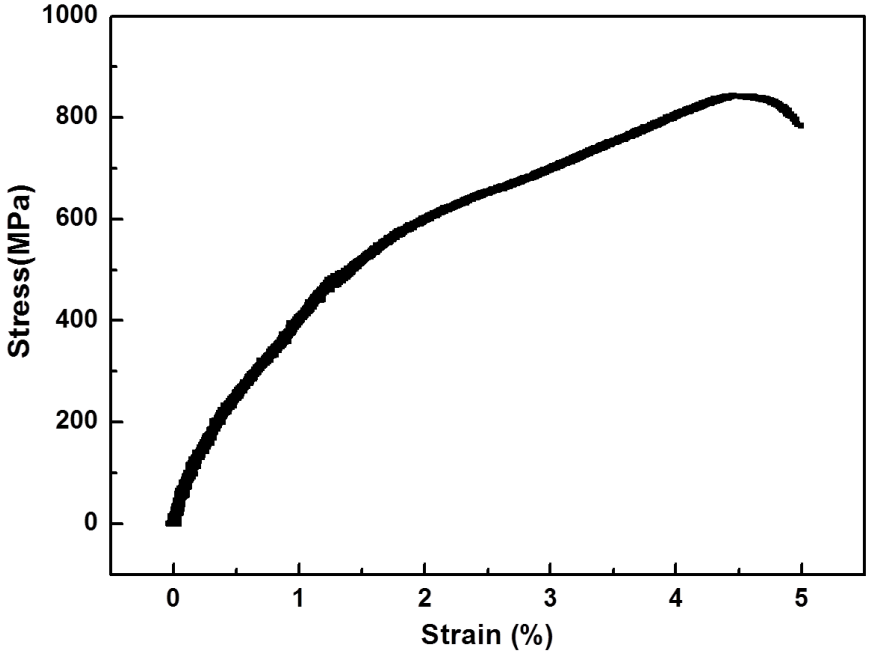

FIG. 6. Compressive stress–strain curve measured at room temperature.